

See discussions, stats, and author profiles for this publication at: <https://www.researchgate.net/publication/239223037>

# $[M(C_5O_5)_2(H_2O)_n]^{2-}$ as a Building Block for Hetero and Homo-bimetallic Coordination Polymers: From 1D Chains to 3D Supramolecular Architectures

ARTICLE in CRYSTAL GROWTH & DESIGN · FEBRUARY 2009

Impact Factor: 4.89 · DOI: 10.1021/cg800827a

---

CITATIONS

7

---

READS

18

10 AUTHORS, INCLUDING:



Chih-Chieh Wang

Soochow University, Taiwan

88 PUBLICATIONS 1,707 CITATIONS

SEE PROFILE



Vladimir E Fedorov

Russian Academy of Sciences

282 PUBLICATIONS 2,478 CITATIONS

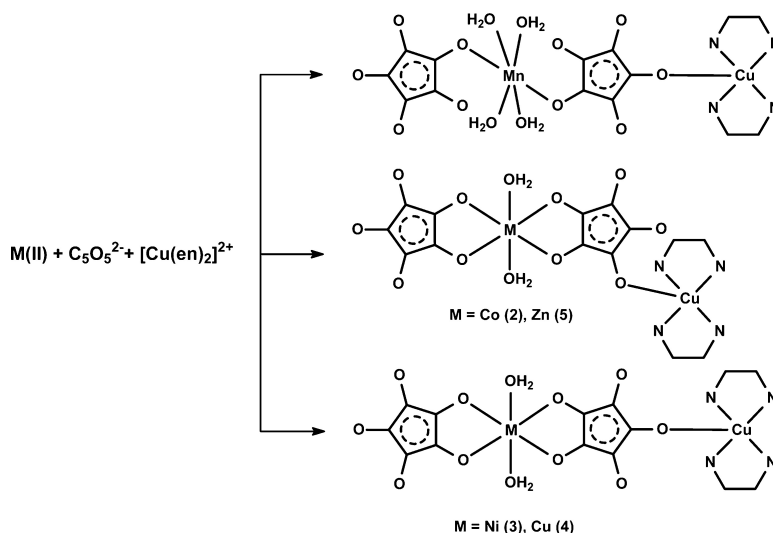
SEE PROFILE

## [M(CO)(HO)] as a Building Block for Hetero- and Homo-bimetallic Coordination Polymers: From 1D Chains to 3D Supramolecular Architectures

Chih-Chieh Wang, Meu-Ju Ke, Cheng-Hsiao Tsai, I-Hsuan Chen, Shin-I Lin, Tzuen-Yeuan Lin, Li-Mei Wu, Gene-Hsiang Lee, Hwo-Shuenn Sheu, and Vladimir E. Fedorov

*Cryst. Growth Des.*, **2009**, 9 (2), 1013-1019 • DOI: 10.1021/cg800827a • Publication Date (Web): 15 December 2008

Downloaded from <http://pubs.acs.org> on February 4, 2009



### More About This Article

Additional resources and features associated with this article are available within the HTML version:

- Supporting Information
- Access to high resolution figures
- Links to articles and content related to this article
- Copyright permission to reproduce figures and/or text from this article

[View the Full Text HTML](#)



ACS Publications  
High quality. High impact.

**[M(C<sub>5</sub>O<sub>5</sub>)<sub>2</sub>(H<sub>2</sub>O)<sub>n</sub>]<sup>2−</sup> as a Building Block for Hetero- and Homo-bimetallic Coordination Polymers: From 1D Chains to 3D Supramolecular Architectures**Chih-Chieh Wang,<sup>\*,†</sup> Meu-Ju Ke,<sup>†</sup> Cheng-Hsiao Tsai,<sup>†</sup> I-Hsuan Chen,<sup>†</sup> Shin-I Lin,<sup>†</sup> Tzuen-Yeuan Lin,<sup>\*,†</sup> Li-Mei Wu,<sup>†</sup> Gene-Hsiang Lee,<sup>‡</sup> Hwo-Shuenn Sheu,<sup>§</sup> and Vladimir E. Fedorov<sup>||</sup>*Department of Chemistry, Soochow University, Taipei, Taiwan, Instrumentation Center, National Taiwan University, Taipei, Taiwan, National Synchrotron Radiation Research Center, Hsinchu 300, Taiwan, and Nikolaev Institute of Inorganic Chemistry, Siberian Branch of the Russian Academy of Sciences, 3 Acad. Lavrentiev pr., Novosilbirk 630090, Russia**Received July 29, 2008; Revised Manuscript Received October 23, 2008*

**ABSTRACT:** A series of one-dimensional (1D) coordination polymers, {[Cu(en)<sub>2</sub>][M(C<sub>5</sub>O<sub>5</sub>)<sub>2</sub>(H<sub>2</sub>O)<sub>m</sub>]·xH<sub>2</sub>O}<sub>n</sub>, (M = Mn (**1**), *m* = 4, *x* = 2; M = Co (**2**), Ni (**3**), Cu (**4**), Zn (**5**), *m* = 2, *x* = 0; en = ethylenediamine; C<sub>5</sub>O<sub>5</sub><sup>2−</sup> = croconate, dianion of 4,5-dihydroxycyclopent-4-ene-1,2,3-trione), using [M(C<sub>5</sub>O<sub>5</sub>)<sub>2</sub>(H<sub>2</sub>O)<sub>n</sub>]<sup>2−</sup> dianion as a building block has been synthesized and characterized by the X-ray diffraction method. Structural determination reveals that, in compounds **1–5**, one [M(C<sub>5</sub>O<sub>5</sub>)<sub>2</sub>(H<sub>2</sub>O)<sub>n</sub>]<sup>2−</sup> dianion coordinates via two oxygen (croconate) donors to the axial sites of two Cu(II) centers of [Cu(en)<sub>2</sub>]<sup>2+</sup> cations to form one-dimensional (1D) linear (**1**, **3** and **4**) or zigzag (**2** and **5**) chains of alternating [M(C<sub>5</sub>O<sub>5</sub>)<sub>2</sub>(H<sub>2</sub>O)<sub>n</sub>]<sup>2−</sup> and [Cu(en)<sub>2</sub>]<sup>2+</sup> units. The croconate acts as a bridging ligand with three coordination modes as μ<sub>1,3</sub>-bismonodentate for **1**, μ<sub>1,2,3</sub>-bidentate/monodentate for **2** and **5**, and μ<sub>1,2,4</sub>-bidentate/monodentate for **3** and **4**, respectively. In addition, a byproduct, [Cu(en)(C<sub>5</sub>O<sub>5</sub>)(H<sub>2</sub>O)]<sub>2</sub> (**6**), which is cocrystallized with **4**, shows a dimeric structure formed through the croconate bridge with μ<sub>1,1,2</sub>-bidentate/monodentate coordination mode. All of their 1D frameworks (**1–5**) and dimeric structure (**6**) are extended to three-dimensional (3D) supramolecular architectures by the intermolecular π–π interaction among croconates and intermolecular hydrogen bonds among the en, croconate, and coordinated water molecules.

**Introduction**

For years, chemists have devoted their efforts to the assembly of coordination polymers by using building units and connecting them.<sup>1–4</sup> The well-known building units are those of cyanometalate anions, [M(CN)<sub>n</sub>]<sup>m−</sup>, which have been extensively used as building units in supramolecular coordination systems.<sup>3,4</sup> They can behave as the bridging moiety to build up high-dimensionality coordination polymers with transition metal cations. Based on the concept, the design of cyanometalate-like building units in the construction of coordination polymers seems to be an important and interesting topic and worth further study. During the past few decades, much research effort has been concentrated on the exploitation of croconate (C<sub>5</sub>O<sub>5</sub><sup>2−</sup>) ligand in the construction of versatile coordination polymeric architectures by using various binding modes. Croconate has been widely used as a polyfunctional ligand, such as hydrogen bonding or π–π interactions, for the construction of extended supramolecular architectures and also used as a bridging ligand with various bonding modes to build up many extended networks.<sup>5–24</sup> It can be coordinated to the metal ions as a terminal bidentate,<sup>5–13</sup> bridging bidentate/modentate (μ<sub>1,2,4</sub>),<sup>5c,6,14,15</sup> bridging bis-bidentate ligand through either four<sup>5c,16,17,18b–d</sup> or three adjacent<sup>5b,d,17–19</sup> croconate-oxygens, bidentate/monodentate plus bridging monodentate,<sup>20</sup> bis-bidentate plus bridging bis-monodentate across four croconate-oxygens,<sup>20</sup> bridging bidentate/modentate (μ<sub>1,2,3</sub>),<sup>21</sup> bis-monodentate,<sup>22</sup> bidentate plus

bridging bis-monodentate through three croconate-oxygens,<sup>23</sup> tris-bidentate through the five croconate-oxygens<sup>18a,18c</sup> and bis-bidentate/monodentate through the five croconate-oxygens.<sup>24</sup> Based on the variety of bonding modes, the croconate ligand resembles more the oxalate ligand and benzene-multicarboxylate ligands, rather than the cyanometallate anions [M(CN)<sub>n</sub>]<sup>m−</sup>, in its scope.<sup>1a,25</sup> In our previous studies,<sup>13</sup> two croconato-complexes, Na<sub>2</sub>[M(C<sub>5</sub>O<sub>5</sub>)<sub>2</sub>(H<sub>2</sub>O)<sub>2</sub>] (M = Ni, Cu), were determined with two terminal bidentate croconate ligands symmetrically bonded to the metal ions. The [M(C<sub>5</sub>O<sub>5</sub>)<sub>2</sub>(H<sub>2</sub>O)<sub>2</sub>]<sup>2−</sup> dianion can be further used as a building block to connect other cationic groups, such as [Cu(en)<sub>2</sub>]<sup>2+</sup> cation, forming polymeric frameworks. Focusing on this issue, we have endeavored to examine the ability of [M(C<sub>5</sub>O<sub>5</sub>)<sub>2</sub>(H<sub>2</sub>O)<sub>n</sub>]<sup>2−</sup> to act as a building block to form hetero- or homo-bimetallic 1D chain-like coordination polymers, {[Cu(en)<sub>2</sub>][M(C<sub>5</sub>O<sub>5</sub>)<sub>2</sub>(H<sub>2</sub>O)<sub>m</sub>]·xH<sub>2</sub>O}<sub>n</sub>, (M = Mn (**1**), *m* = 4, *x* = 2; M = Co (**2**), Ni (**3**), Cu (**4**), Zn (**5**), *m* = 2, *x* = 0; C<sub>5</sub>O<sub>5</sub><sup>2−</sup> = croconate, dianion of 4,5-dihydroxycyclopent-4-ene-1,2,3-trione; en = ethylenediamine), with μ<sub>1,3</sub>-bismonodentate, μ<sub>1,2,3</sub>-bidentate/monodentate, and μ<sub>1,2,4</sub>-bidentate/monodentate bridging modes of croconate ligands (Scheme 1). Furthermore, these 1D chains are then extended to 3D supramolecular architectures via hydrogen bonding and π–π interactions by the polyfunctional croconate ligands.

**Experimental Section**

**General Procedures and Physical Measurements.** All chemicals were of reagent grade and were used as commercially obtained without further purification. Infrared spectra were measured on a Nicolet Fourier Transform IR, MAGNA-IR 500 spectrometer in the range of 500–4000 cm<sup>−1</sup> using the KBr disk technique. Thermogravimetric analyses (TGA) of these compounds were performed on a computer-controlled Perkin-Elmer 7 Series/UNIX TGA7 analyzer. Single-phased powder samples were loaded into alumina pans and heated with a ramp rate of 5 °C/

\* To whom correspondence should be addressed. Fax: 886-2-28811053; tel.: 886-2-28819471 ext 6824; e-mail: ccwang@scu.edu.tw.

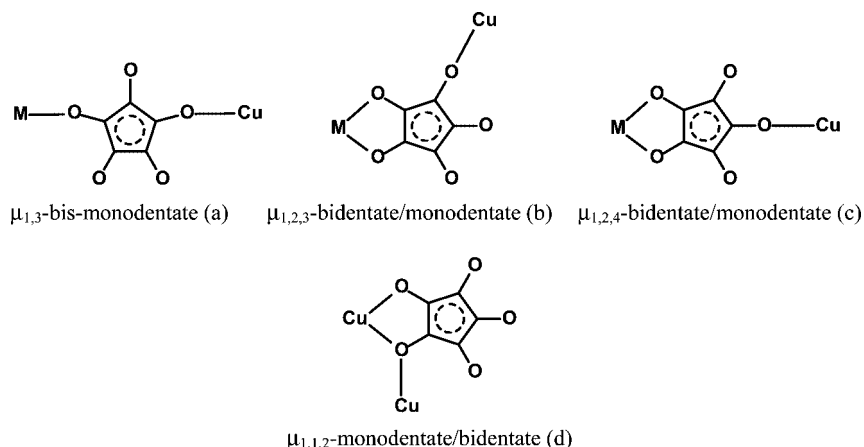
<sup>†</sup> Soochow University.

<sup>‡</sup> National Taiwan University.

<sup>§</sup> National Synchrotron Radiation Research Center.

<sup>||</sup> Nikolaev Institute of Inorganic Chemistry, Siberian Branch of the Russian Academy of Sciences.

Scheme 1. Bridging Modes of Croconate Shown in Compounds 1–6



min from room temperature to 800 °C under nitrogen atmosphere. The elemental analyses of carbon, hydrogen, and nitrogen were determined with a Perkin-Elmer model 2400 Series II Analyzer. In situ powder X-ray diffraction was performed at the beamline BL01C2 of the National Synchrotron Radiation Research Center (NSRRC) Taiwan. The synchrotron ring energy is 1.5 GeV with a current of 300 mA. The X-ray wavelength was 1.0332 Å which delivered by a Si(111) double crystal monochromator. The powder samples were sealed in 1 mm quartz capillary and heated under hot air stream from room temperature up to 600 °C during the in situ XRD measurement. Two dimensional powder X-ray diffraction patterns were recorded by using Mar345 imaging plate detector with a pixel size of 100  $\mu$ m and a typical exposure time of 2 min. The sample to imaging plate distance was ca. 300 mm and the diffraction angle was calibrated by the standard powders of Ag-Behenate and Si powder (NBS640b). The one-dimensional XRD profile was converted using the FIT2D program.

**[Cu(en)<sub>2</sub>][Mn(C<sub>5</sub>O<sub>5</sub>)<sub>2</sub>(H<sub>2</sub>O)<sub>4</sub>]·2H<sub>2</sub>O (1).** To a 2.0 mL aqueous solution of MnCl<sub>2</sub>·4H<sub>2</sub>O (9.9 mg, 0.05 mmol) was added a 2.0 mL of Na<sub>2</sub>C<sub>5</sub>O<sub>5</sub> (0.1 mmol). While stirring, a 0.20 mL deep blue aqueous solution of [Cu(en)<sub>2</sub>]Cl<sub>2</sub> (0.05 mmol) was added dropwise to this solution. The resulting brown solution was covered and left undisturbed to yield X-ray quality, brown crystals of [Cu(en)<sub>2</sub>]-[Mn(C<sub>5</sub>O<sub>5</sub>)<sub>2</sub>(H<sub>2</sub>O)<sub>4</sub>]·2H<sub>2</sub>O (1) over one week. Yield: 0.0210 g (69%). Anal. Calcd for C<sub>14</sub>H<sub>28</sub>N<sub>4</sub>O<sub>16</sub>CuMn: C, 27.61; H, 4.30; N, 9.20. Found: C, 26.95; H, 3.91; N, 9.00. IR (KBr) IR (KBr pellet):  $\nu$  = 3371, 3260, 1671, 1626, 1588, 1538, 1454, 1377, 1325, 1041, 706, 532 cm<sup>-1</sup>.

**[Cu(en)<sub>2</sub>][Co(C<sub>5</sub>O<sub>5</sub>)<sub>2</sub>(H<sub>2</sub>O)<sub>2</sub>] (2).** To a 2.0 mL aqueous solution of CoCl<sub>2</sub> (6.5 mg, 0.05 mmol) was added a 2.0 mL of Na<sub>2</sub>C<sub>5</sub>O<sub>5</sub> (0.1 mmol). While stirring, a 0.20 mL deep blue aqueous solution of [Cu(en)<sub>2</sub>]Cl<sub>2</sub> (0.05 mmol) was added dropwise to this solution. The resulting purple solution was covered and left undisturbed to yield X-ray quality, black crystals of [Cu(en)<sub>2</sub>][Co(C<sub>5</sub>O<sub>5</sub>)<sub>2</sub>(H<sub>2</sub>O)<sub>2</sub>] (2) over three days. Yield: 0.0191 g (68%). Anal. Calcd for C<sub>14</sub>H<sub>20</sub>N<sub>4</sub>O<sub>12</sub>CuCo: C, 30.09; H, 3.61; N, 10.03. Found: C, 29.74; H, 3.30; N, 10.11. IR (KBr pellet):  $\nu$  = 3332, 3275, 1712, 1673, 1599, 1548, 1539, 1515, 1511, 1506, 1472, 1451, 1374, 1321, 1032, 715, 534 cm<sup>-1</sup>.

**[Cu(en)<sub>2</sub>][Ni(C<sub>5</sub>O<sub>5</sub>)<sub>2</sub>(H<sub>2</sub>O)<sub>2</sub>] (3).** To a 2.0 mL aqueous solution of NiCl<sub>2</sub>·6H<sub>2</sub>O (11.9 mg, 0.05 mmol) was added a 2.0 mL of Na<sub>2</sub>C<sub>5</sub>O<sub>5</sub> (0.1 mmol). While stirring, a 0.20 mL deep blue aqueous solution of [Cu(en)<sub>2</sub>]Cl<sub>2</sub> (0.05 mmol) was added dropwise to this solution. The resulting blue solution was covered and left undisturbed to yield X-ray quality, brown crystals of [Cu(en)<sub>2</sub>][Ni(C<sub>5</sub>O<sub>5</sub>)<sub>2</sub>(H<sub>2</sub>O)<sub>2</sub>] (2) over three days. Yield: 0.0175 g (63%). Anal. Calcd for C<sub>14</sub>H<sub>20</sub>N<sub>4</sub>O<sub>12</sub>CuNi: C, 30.20; H, 3.62; N, 10.06. Found: C, 30.24; H, 2.78; N, 10.20. IR (KBr pellet):  $\nu$  = 3335, 3247, 1711, 1661, 1634, 1593, 1520, 1451, 1374, 1321, 1033, 712, 535 cm<sup>-1</sup>.

**[Cu(en)<sub>2</sub>][Cu(C<sub>5</sub>O<sub>5</sub>)<sub>2</sub>(H<sub>2</sub>O)<sub>2</sub>] (4) and [Cu(en)(C<sub>5</sub>O<sub>5</sub>)(H<sub>2</sub>O)]<sub>2</sub> (6).** To a 2.0 mL aqueous solution of CuCl<sub>2</sub>·2H<sub>2</sub>O (8.5 mg, 0.05 mmol) was added a 2.0 mL of Na<sub>2</sub>C<sub>5</sub>O<sub>5</sub> (0.1 mmol). While stirring, a 0.20 mL deep blue aqueous solution of [Cu(en)<sub>2</sub>]Cl<sub>2</sub> (0.05 mmol) was added dropwise to this solution. The resulting green solution was covered and left undisturbed to yield X-ray quality, red and green crystals of [Cu(en)<sub>2</sub>][Cu(C<sub>5</sub>O<sub>5</sub>)<sub>2</sub>(H<sub>2</sub>O)<sub>2</sub>] (4) and [Cu(en)(C<sub>5</sub>O<sub>5</sub>)(H<sub>2</sub>O)]<sub>2</sub> (6), respectively, over one week. Yield: 4, 0.0170 g (60%) and 6, 0.0093 g (33%). Anal. Calcd for 4, C<sub>14</sub>H<sub>20</sub>N<sub>4</sub>O<sub>12</sub>Cu<sub>2</sub>: C, 29.85; H, 3.58; N, 9.94. Found:

C, 29.83; H, 3.42; N, 10.02. IR (KBr pellet):  $\nu$  = 3333, 3217, 3263, 2950, 2888, 1722, 1662, 1638, 1598, 1582, 1538, 1531, 1526, 1470, 1465, 1443, 1361, 1310, 1276, 1039, 707, 535 cm<sup>-1</sup>. Anal. Calcd for 6, C<sub>14</sub>H<sub>20</sub>N<sub>4</sub>O<sub>12</sub>Cu<sub>2</sub>: C, 29.85; H, 3.58; N, 9.94. Found: C, 29.14; H, 3.36; N, 9.84. IR (KBr pellet):  $\nu$  = 3420, 3333, 3235, 1716, 1644, 1603, 1569, 1505, 1488, 1465, 1454, 1396, 1368, 1321, 1055, 719, 538 cm<sup>-1</sup>.

**[Cu(en)<sub>2</sub>][Zn(C<sub>5</sub>O<sub>5</sub>)<sub>2</sub>(H<sub>2</sub>O)<sub>2</sub>] (5).** To a 2.0 mL aqueous solution of ZnCl<sub>2</sub> (6.8 mg, 0.05 mmol) was added a 2.0 mL of Na<sub>2</sub>C<sub>5</sub>O<sub>5</sub> (0.1 mmol). While stirring, a 0.20 mL deep blue aqueous solution of [Cu(en)<sub>2</sub>]Cl<sub>2</sub> (0.05 mmol) was added dropwise to this solution. The resulting blue solution was covered and left undisturbed to yield X-ray quality, brown crystals of [Cu(en)<sub>2</sub>][Zn(C<sub>5</sub>O<sub>5</sub>)<sub>2</sub>(H<sub>2</sub>O)<sub>2</sub>] (5) over three days. Yield: 0.0143 g (51%). Anal. Calcd for C<sub>14</sub>H<sub>20</sub>N<sub>4</sub>O<sub>12</sub>CuNi: C, 29.75; H, 3.57; N, 9.91. Found: C, 29.90; H, 3.56; N, 10.03. IR (KBr pellet):  $\nu$  = 3331, 3283, 3244, 1742, 1713, 1664, 1563, 1557, 1548, 1544, 1539, 1532, 1506, 1454, 1373, 1335, 1277, 1035, 695, 533 cm<sup>-1</sup>.

**Crystallographic Data Collection and Refinement.** Single-crystal structure analyses of compounds 1–6 were performed on a Siemens SMART diffractometer with a CCD detector with Mo radiation ( $\lambda$  = 0.71073 Å) at room temperature. A preliminary orientation matrix and unit cell parameters were determined from 3 runs of 15 frames each, each frame corresponding to a 0.3° scan in 10 s, followed by spot integration and least-squares refinement. For each structure, data were measured using  $\omega$  scans of 0.3° per frame for 20 s until a complete hemisphere had been collected. Cell parameters were retrieved using SMART<sup>26a</sup> software and refined with SAINT<sup>26b</sup> on all observed reflections. Data reduction was performed with the SAINT<sup>26b</sup> software and corrected for Lorentz and polarization effects. Absorption corrections were applied with the program SADABS.<sup>27</sup> Direct phase determination and subsequent difference Fourier map synthesis yielded the positions of all non-hydrogen atoms, which were subjected to anisotropic refinements. For compounds 1–6, all hydrogen atoms were generated geometrically (C–H = 0.97 Å and N–H = 0.90 Å) with the exception of the hydrogen atoms of the coordinated and solvated water molecules, which were located in the difference Fourier map with the corresponding positions and isotropic displacement parameters being refined and then constrained to O–H = 0.95 Å. The final full-matrix, least-squares refinement on  $F^2$  was applied for all observed reflections [ $I > 2\sigma(I)$ ]. All calculations were performed using the SHELXTL-PC V 5.03 software package.<sup>28</sup> Crystallographic data and details of data collections and structure refinements of 1–6 are listed in Table 1.

CCDC for 1–6 contains the supplementary crystallographic data for this paper. These data can be obtained free of charge at [www.ccdc.cam.ac.uk/conts/retrieving.html](http://www.ccdc.cam.ac.uk/conts/retrieving.html) [or from the Cambridge Crystallographic Data Centre, 12, Union Road, Cambridge CB2 1EZ, UK; fax: (Internet.) +44-1223/336-033; E-mail: [deposit@ccdc.cam.ac.uk](mailto:deposit@ccdc.cam.ac.uk)].

## Results and Discussion

**Synthesis and Spectral Studies.** The supramolecular assemblies of compounds 1–6 were synthesized via the same synthetic procedure by the reactions of anhydrous or hydrated

**Table 1.** Crystal Data and Structural Refinement for Compounds 1–6

	1	2	3
formula	C <sub>14</sub> H <sub>28</sub> MnCuN <sub>4</sub> O <sub>16</sub>	C <sub>14</sub> H <sub>20</sub> CoCuN <sub>4</sub> O <sub>12</sub>	C <sub>14</sub> H <sub>20</sub> NiCuN <sub>4</sub> O <sub>12</sub>
fw	626.88	558.81	558.57
cryst syst	monoclinic	triclinic	monoclinic
space group	<i>P</i> 2 <sub>1</sub> / <i>c</i>	<i>P</i> $\bar{1}$	<i>P</i> 2 <sub>1</sub> / <i>c</i>
<i>a</i> (Å)	13.0699(7)	7.1591(2)	9.8755(5)
<i>b</i> (Å)	13.0660(7)	8.4702(2)	13.9423(9)
<i>c</i> (Å)	7.0103(4)	9.3530(2)	7.0743(4)
$\alpha$ (deg)	90.0	101.792(1)	90.0
$\beta$ (deg)	101.104(1)	106.691(1)	98.677(1)
$\gamma$ (deg)	90.0	109.665(1)	90.0
<i>V</i> (Å <sup>3</sup> )	1174.75(11)	482.25(2)	962.89(10)
<i>Z</i>	2	1	2
<i>D</i> <sub>calc</sub> (g/cm <sup>3</sup> )	1.772	1.924	1.927
$\mu$ (mm <sup>-1</sup> )	1.528	2.039	2.158
<i>F</i> (000)	644	284	570
reflns collected	11456	8733	9397
unique reflns ( <i>I</i> > 2 $\sigma$ ( <i>I</i> ))	2262	1851	1967
max and min trans	0.9556, 0.8032	0.8250, 0.7430	0.8131, 0.5637
<i>R</i> <sub>1</sub> , <i>wR</i> <sub>2</sub> <sup>a</sup> ( <i>I</i> > 2 $\sigma$ ( <i>I</i> ))	0.0391, 0.0999	0.0449, 0.1322	0.0482, 0.1033
<i>R</i> <sub>1</sub> , <i>wR</i> <sub>2</sub> <sup>a</sup> (all data)	0.0490, 0.1129	0.0548, 0.1382	0.0561, 0.1067
GOF on <i>F</i> <sup>2</sup>	1.077	1.079	1.190
no. of variable	184	157	172

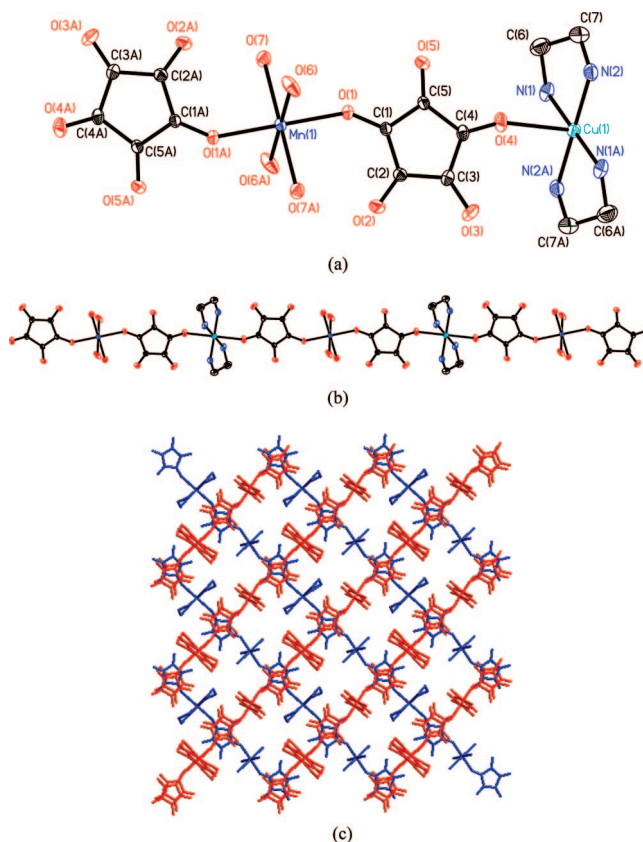
  

	4	5	6
formula	C <sub>14</sub> H <sub>20</sub> Cu <sub>2</sub> N <sub>4</sub> O <sub>12</sub>	C <sub>14</sub> H <sub>20</sub> ZnCuN <sub>4</sub> O <sub>12</sub>	C <sub>14</sub> H <sub>20</sub> Cu <sub>2</sub> N <sub>4</sub> O <sub>12</sub>
fw	563.42	565.25	563.42
cryst syst	monoclinic	triclinic	triclinic
space group	<i>P</i> 2 <sub>1</sub> / <i>c</i>	<i>P</i> $\bar{1}$	<i>P</i> $\bar{1}$
<i>a</i> (Å)	10.0074(3)	7.2193(9)	7.5537(3)
<i>b</i> (Å)	13.9437(4)	8.4640(10)	8.0458(3)
<i>c</i> (Å)	7.0100(2)	9.3642(11)	9.1444(3)
$\alpha$ (deg)	90.0	101.239(2)	112.811(1)
$\beta$ (deg)	98.075(1)	106.892(2)	103.164(1)
$\gamma$ (deg)	90.0	110.011(2)	99.505(1)
<i>V</i> (Å <sup>3</sup> )	968.48(5)	486.10(10)	478.53(3)
<i>Z</i>	2	1	1
<i>D</i> <sub>calc</sub> (g/cm <sup>3</sup> )	1.932	1.931	1.955
$\mu$ (mm <sup>-1</sup> )	2.272	2.403	2.299
<i>F</i> (000)	572	287	286
reflns collected	8531	6201	5778
unique reflns ( <i>I</i> > 2 $\sigma$ ( <i>I</i> ))	1624	1914	1871
max and min trans	0.7456, 0.6257	0.7951, 0.5849	0.7460, 0.6540
<i>R</i> <sub>1</sub> , <i>wR</i> <sub>2</sub> <sup>a</sup> ( <i>I</i> > 2 $\sigma$ ( <i>I</i> ))	0.0250, 0.0639	0.0355, 0.0862	0.0250, 0.0555
<i>R</i> <sub>1</sub> , <i>wR</i> <sub>2</sub> <sup>a</sup> (all data)	0.0407, 0.0684	0.0424, 0.0893	0.0335, 0.0569
GOF on <i>F</i> <sup>2</sup>	1.010	1.114	1.087
no. of variable	173	156	185

$$^a R_F = \sum |F_o - F_c| / \sum |F_o|; R_w(F^2) = [\sum w(F_o^2 - F_c^2)^2 / \sum w(F_o^4)]^{1/2}.$$

MCl<sub>2</sub>·*n*H<sub>2</sub>O (*M* = Mn, Co, Ni, Cu, Zn), Na<sub>2</sub>C<sub>5</sub>O<sub>5</sub> and [Cu(en)<sub>2</sub>Cl<sub>2</sub>] in a 1:2:1 molar ratio. The synthetic reproducibility is very nice. The most relevant IR features are those associated with the chelating croconate ligands. Strong and broad absorptions occurring in the range of 1610–1350 cm<sup>-1</sup> centered at 1538, 1511, 1520, 1531, 1532, and 1488 cm<sup>-1</sup> for **1**, **2**, **3**, **4**, **5**, and **6**, respectively, are characteristic of the salts of C<sub>n</sub>O<sub>n</sub><sup>2-</sup> ions,<sup>29</sup> and in the present cases they can be assigned to vibrational modes representing mixtures of C–O and C–C stretching motions. The presence of medium-strength absorptions at 1626 and 1588 cm<sup>-1</sup> for **1**, 1673 and 1599 cm<sup>-1</sup> for **2**, 1634 and 1593 cm<sup>-1</sup> for **3**, 1638 and 1582 cm<sup>-1</sup> for **4**, 1664 and 1599 cm<sup>-1</sup> for **5**, and 1644 and 1603 cm<sup>-1</sup> for **6** may be assigned to the coordinated carbonyl group. Additional weak bands are observed above 1700 cm<sup>-1</sup> (1700 cm<sup>-1</sup> for **1**, 1712 cm<sup>-1</sup> for **2**, 1711 cm<sup>-1</sup> for **3**, 1713 cm<sup>-1</sup> for **4**, 1713 cm<sup>-1</sup> for **5**, and 1716 cm<sup>-1</sup> for **6**), which may be taken as evidence for the presence of uncoordinated carbonyl groups of croconate ligand.

**Structural Characterization of Compounds 1–6.** [Cu(en)<sub>2</sub>][Mn(C<sub>5</sub>O<sub>5</sub>)<sub>2</sub>(H<sub>2</sub>O)<sub>4</sub>]·2H<sub>2</sub>O (**1**). A perspective view of compound **1** with the atom numbering scheme is shown in



**Figure 1.** (a) ORTEP drawing for the asymmetric unit of [Cu(en)<sub>2</sub>][Mn(C<sub>5</sub>O<sub>5</sub>)<sub>2</sub>(H<sub>2</sub>O)<sub>4</sub>]·2H<sub>2</sub>O (**1**), showing 30% probability ellipsoids. Solvated water molecules were omitted for clarity. Symmetry code: (A) =  $-x, -y, -z$  for N(1), N(2); (A) =  $-x + 1, -y + 1, -z$  for O(1), O(6), O(7). (b) The 1D linear chain is formed by the croconate bridge with a  $\mu_{1,3}$ -bis-monodentate coordination mode. (c) A view of the 2D sheets arranged in an ABAB... packing pattern and extended to infinite 3D cross-like-array network.

**Table 2.** Selected Bond Lengths (Å) and Angles (°) for **1**<sup>a</sup>

Mn(1)–O(1)	2.135(2)	Cu(1)–N(1)	2.003(2)
Mn(1)–O(6)	2.143(2)	Cu(1)–N(2)	2.005(2)
Mn(1)–O(7)	2.238(2)	Cu(1)–O(4)	2.492(2)
N(1)–Cu(1)–N(1A)	180	N(1)–Cu(1)–N(2A)	95.0(1)
N(1)–Cu(1)–N(2)	85.0(1)	N(2)–Cu(1)–N(2A)	180
O(1)–Mn(1)–O(1A)	180	O(1)–Mn(1)–O(7A)	93.98(7)
O(1)–Mn(1)–O(6A)	89.21(8)	O(6)–Mn(1)–O(7A)	95.05(9)
O(1)–Mn(1)–O(6)	90.79(8)	O(6)–Mn(1)–O(7)	84.95(9)
O(6)–Mn(1)–O(6A)	180	O(1)–Mn(1)–O(7)	86.02(7)
O(7A)–Mn(1)–O(7)	180		

<sup>a</sup> Symmetry code: (A) =  $-x, -y, -z$  for N(1), N(2); (A) =  $-x + 1, -y + 1, -z$  for O(1), O(6), O(7).

Figure 1a. The selected bond distances and angles with their estimated standard derivations around the Mn(II) and Cu(II) ions are listed in Table 2. The asymmetric unit of **1** consists of a half of a [Mn(C<sub>5</sub>O<sub>5</sub>)<sub>2</sub>(H<sub>2</sub>O)<sub>4</sub>]<sup>2-</sup> anion, half of a planar [Cu(en)<sub>2</sub>]<sup>2+</sup> cation, and a water molecule. The Mn<sup>II</sup> and Cu<sup>II</sup> ions are both located at the inversion center of (0.5, 0.5, 0) and (0, 0, 0), respectively. Two croconate oxygens of [Mn(C<sub>5</sub>O<sub>5</sub>)<sub>2</sub>(H<sub>2</sub>O)<sub>4</sub>]<sup>2-</sup> (O(4) and O(4)\* (\* indicates a symmetry operation of  $-x + 1, -y + 1, -z$ ) coordinate to adjacent [Cu(en)<sub>2</sub>]<sup>2+</sup> cations forming a 1D linear chain (Figure 1b) of alternating [Cu(en)<sub>2</sub>]<sup>2+</sup> and [Mn(C<sub>5</sub>O<sub>5</sub>)<sub>2</sub>(H<sub>2</sub>O)<sub>4</sub>]<sup>2-</sup> units running along the [1, 1, 0] or [1,  $\bar{1}$ , 0] directions. The arrangement of these 1D linear chains in the lattice is depicted in Figure 1c. The croconate acts a bridging ligand with a unprecedented  $\mu_{1,3}$ -bis-monodentate<sup>22</sup> coordination



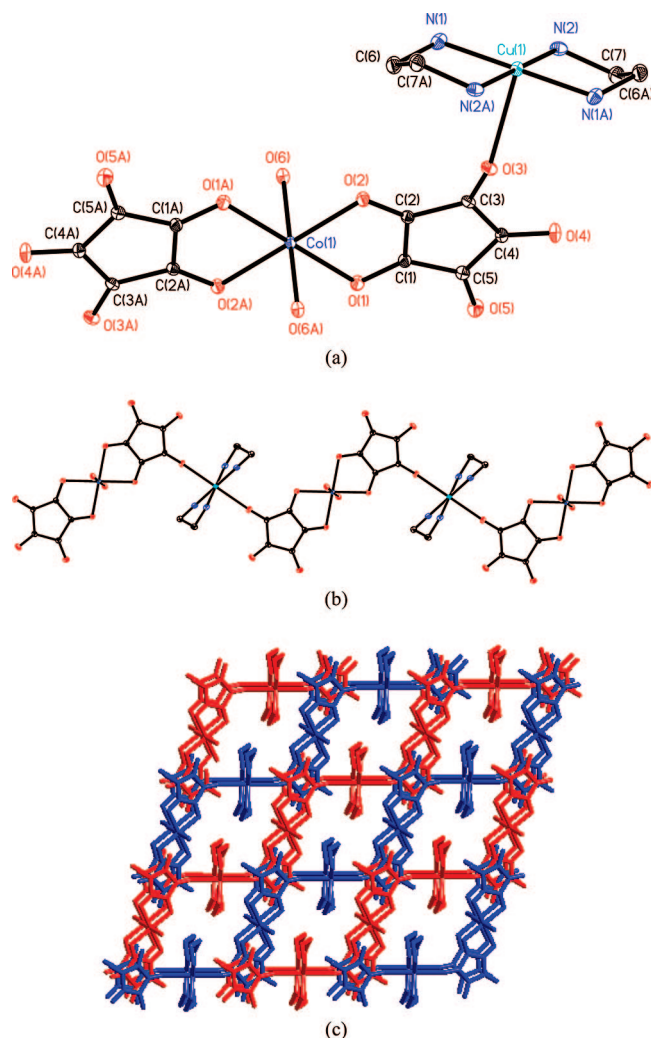


**Figure 2.** (a) ORTEP drawing for the asymmetric unit of  $[\text{Cu}(\text{en})_2][\text{Co}(\text{C}_5\text{O}_5)_2(\text{H}_2\text{O})_2]$ , showing 30% probability ellipsoids. Symmetry code: (A) =  $-x, -y, -z$  for N(1), N(2); (A) =  $-x, -y - 1, -z + 1$  for O(1), O(2), and O(6). (b) The 1D zigzag chain is formed by the croconate bridge with a  $\mu_{1,2,3}$ -bidentate/monodentate coordination mode. (c) A view of the 2D sheets arranged in an ABAB... packing pattern and extended to infinite 3D cross-like-array network.

mode (Scheme 1a) connecting the  $\text{Mn}^{\text{II}}$  and  $\text{Cu}^{\text{II}}$  centers with the intrachain  $\text{Mn} \cdots \text{Cu}$  separation being 9.24 Å. The  $\text{Cu}^{\text{II}}$  ion has a nearly octahedral surrounding showing a elongation along the croconate bound axial positions with  $\text{Cu}-\text{O}(4) = 2.492(2)$  Å.

**$[\text{Cu}(\text{en})_2][\text{M}(\text{C}_5\text{O}_5)_2(\text{H}_2\text{O})_2]$ ,  $\text{M} = \text{Co}$  (2),  $\text{Zn}$  (5).** The X-ray determination reveals that compounds **2** and **5** are isostructural and their perspective view with the atom numbering scheme is shown in Figure 2a as an example of **2**. The selected bond distances and angles with their estimated standard derivations around the metal ions are listed in Table 3. The asymmetric unit of **2** and **5** consists of a half of a  $[\text{M}(\text{C}_5\text{O}_5)_2(\text{H}_2\text{O})_4]^{2-}$  anion ( $\text{M} = \text{Co}$  (2) and  $\text{Zn}$  (5)) and half of a planar  $[\text{Cu}(\text{en})_2]^{2+}$  cation. The  $\text{M}^{\text{II}}$  and  $\text{Cu}^{\text{II}}$  ions are both located at the inversion center of (0.0,  $-0.5$ , 0.5) and (0, 0, 0), respectively. Two croconate oxygens of  $[\text{M}(\text{C}_5\text{O}_5)_2(\text{H}_2\text{O})_2]^{2-}$  (O(3) and O(3)\* (\* indicates a symmetry operation of  $-x, -y, -z$ ) coordinate to adjacent  $[\text{Cu}(\text{en})_2]^{2+}$  cations forming a 1D zigzag chain of alternating  $[\text{Cu}(\text{en})_2]^{2+}$  and  $[\text{M}(\text{C}_5\text{O}_5)_2(\text{H}_2\text{O})_2]^{2-}$  units running along the  $[0, 1, \bar{1}]$  directions (Figure 2b). The arrangement of these 1D zigzag chains in the lattice is depicted in Figure 2c. The croconate acts

**Table 3.** Selected Bond Lengths (Å) and Angles (°) for **2** and **5**<sup>a</sup>

2		5	
$\text{Cu}(1)-\text{N}(1)$	2.018(4)	$\text{Cu}(1)-\text{N}(1)$	2.010(2)
$\text{Cu}(1)-\text{N}(2)$	2.018(4)	$\text{Cu}(1)-\text{N}(2)$	2.011(2)
$\text{Cu}(1)-\text{O}(3)$	2.496(3)	$\text{Cu}(1)-\text{O}(3)$	2.523(2)
$\text{Co}(1)-\text{O}(1)$	2.133(3)	$\text{Zn}(1)-\text{O}(1)$	2.165(2)
$\text{Co}(1)-\text{O}(2)$	2.142(3)	$\text{Zn}(1)-\text{O}(2)$	2.116(2)
$\text{Co}(1)-\text{O}(6)$	2.050(3)	$\text{Zn}(1)-\text{O}(6)$	2.055(2)
$\text{N}(1)-\text{Cu}(1)-\text{N}(1\text{A})$	180	$\text{N}(1)-\text{Cu}(1)-\text{N}(1\text{A})$	180
$\text{N}(1)-\text{Cu}(1)-\text{N}(2\text{A})$	84.8(2)	$\text{N}(1)-\text{Cu}(1)-\text{N}(2\text{A})$	84.8(1)
$\text{N}(1)-\text{Cu}(1)-\text{N}(2)$	95.2(2)	$\text{N}(1)-\text{Cu}(1)-\text{N}(2)$	95.2(1)
$\text{N}(2)-\text{Cu}(1)-\text{N}(2\text{A})$	180	$\text{N}(2)-\text{Cu}(1)-\text{N}(2\text{A})$	180
$\text{O}(6)-\text{Co}(1)-\text{O}(6\text{A})$	180	$\text{O}(6)-\text{Zn}(1)-\text{O}(6\text{A})$	180
$\text{O}(6)-\text{Co}(1)-\text{O}(1)$	92.3(1)	$\text{O}(6)-\text{Zn}(1)-\text{O}(1)$	91.26(9)
$\text{O}(6)-\text{Co}(1)-\text{O}(1\text{A})$	87.7(1)	$\text{O}(6)-\text{Zn}(1)-\text{O}(1\text{A})$	88.74(9)
$\text{O}(1)-\text{Co}(1)-\text{O}(1\text{A})$	180	$\text{O}(1)-\text{Zn}(1)-\text{O}(1\text{A})$	180
$\text{O}(6)-\text{Co}(1)-\text{O}(2\text{A})$	91.4(1)	$\text{O}(6)-\text{Zn}(1)-\text{O}(2\text{A})$	92.53(8)
$\text{O}(1)-\text{Co}(1)-\text{O}(2\text{A})$	98.8(1)	$\text{O}(1)-\text{Zn}(1)-\text{O}(2\text{A})$	98.75(7)
$\text{O}(6)-\text{Co}(1)-\text{O}(2)$	88.6(1)	$\text{O}(6)-\text{Zn}(1)-\text{O}(2)$	87.47(8)
$\text{O}(1)-\text{Co}(1)-\text{O}(2)$	81.2(1)	$\text{O}(1)-\text{Zn}(1)-\text{O}(2)$	81.25(7)
$\text{O}(2)-\text{Co}(1)-\text{O}(2\text{A})$	180	$\text{O}(2)-\text{Zn}(1)-\text{O}(2\text{A})$	180

<sup>a</sup> Symmetry code: (A) =  $-x, -y, -z$  for N(1), N(2); (A) =  $-x, -y - 1, -z + 1$  for O(1), O(2), and O(6).

a bridging ligand with a  $\mu_{1,2,3}$ -bidentate/monodentate<sup>21</sup> coordination mode (Scheme 1b) connecting the  $\text{M}^{\text{II}}$  and  $\text{Cu}^{\text{II}}$  centers with the intrachain  $\text{Co} \cdots \text{Cu}$  (**2**) and  $\text{Zn} \cdots \text{Cu}$  (**5**) separations being 6.921 and 6.896 Å, respectively. The  $\text{Cu}^{\text{II}}$  ion has a nearly octahedral surrounding showing a elongation along the croconate bound axial positions with  $\text{Cu}-\text{O}(3) = 2.496(3)$  and  $2.523(2)$  Å for **2** and **5**, respectively.

**$[\text{Cu}(\text{en})_2][\text{M}(\text{C}_5\text{O}_5)_2(\text{H}_2\text{O})_2]$ ,  $\text{M} = \text{Ni}$  (3),  $\text{Cu}$  (4).** The X-ray determination reveals that compounds **3** and **4** are isostructural and their perspective view with the atom numbering scheme is shown in Figure 3a as an example of **3**. The selected bond distances and angles with their estimated standard derivations around the metal ions are listed in Table 4. The asymmetric unit of **3** and **4** consists of a half of a  $[\text{M}(\text{C}_5\text{O}_5)_2(\text{H}_2\text{O})_4]^{2-}$  anion ( $\text{M} = \text{Ni}$  and  $\text{Cu}$ ) and half of a planar  $[\text{Cu}(\text{en})_2]^{2+}$  cation. The  $\text{M}^{\text{II}}$  and  $\text{Cu}^{\text{II}}$  ions are both located at the inversion center of (0.5, 0.5, 0.5) and (1.0, 0.0, 0.5), respectively. Two croconate oxygens of  $[\text{M}(\text{C}_5\text{O}_5)_2(\text{H}_2\text{O})_2]^{2-}$  (O(4) and O(4)\* (\* indicates a symmetry operation of  $2 - x, -y, 1 - z$ ) coordinate to adjacent  $[\text{Cu}(\text{en})_2]^{2+}$  cations forming a 1D linear chain (Figure 3b) of alternating  $[\text{Cu}(\text{en})_2]^{2+}$  and  $[\text{M}(\text{C}_5\text{O}_5)_2(\text{H}_2\text{O})_2]^{2-}$  units running along the  $[1, 1, 0]$  and  $[1, \bar{1}, 0]$  directions. The arrangement of these 1D linear chains in the lattice is depicted in Figure 3c. The croconate acts a bridging ligands with a  $\mu_{1,2,4}$ -bidentate/monodentate<sup>5c,6,14,15</sup> coordination mode (Scheme 1c) connecting the  $\text{M}^{\text{II}}$  and  $\text{Cu}^{\text{II}}$  centers with the intrachain  $\text{M} \cdots \text{Cu}$  separation being 8.543 and 8.582 Å for **3** and **4**, respectively. The  $\text{Cu}^{\text{II}}$  ion has a nearly octahedral surrounding showing elongation along the croconate bound axial positions with  $\text{Cu}-\text{O}(3) = 2.512(3)$  and  $2.491(2)$  Å for **3** and **4**, respectively.

The most remarkable and interesting features on the construction of their 3D supramolecular architectures in compounds **1–5** is that the subtle combination of  $\pi \cdots \pi$  stacking and hydrogen-bonding interactions serves to connect these 1D coordination linear (**1**, **3** and **4**) or zigzag (**2** and **5**) chains to a 3D cross-like array as shown in Figures 1c, 2c, and 3c for **1**, **2** and **5**, **3** and **4**, respectively. First, the nearly cross-like arrangement and the well-coplanarity of these 1D polymeric chains are responsible for the occurrence of the  $\pi \cdots \pi$  stacking interactions between the alternate polymeric chains. The distances between the ring centroids of the croconate rings of alternate chains are 3.666 Å in **1**, 3.589, 3.758 Å in **2**, 3.648 Å in **3**, 3.601 Å in **4** and 3.608, 3.809 Å in **5**, respectively (Table 5), all falling in the general

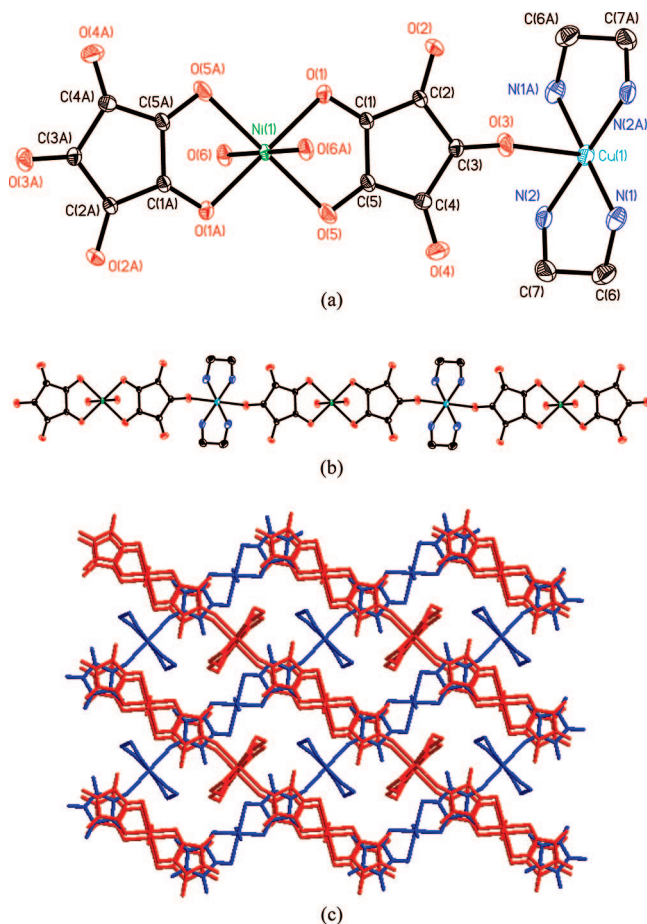


**Figure 3.** (a) ORTEP drawing for the asymmetric unit of [Cu(en)<sub>2</sub>][Ni(C<sub>5</sub>O<sub>5</sub>)<sub>2</sub>(H<sub>2</sub>O)<sub>2</sub>], showing 30% probability ellipsoids. Symmetry code: (A) =  $-x + 2, -y, -z + 1$  for N(1) and N(2); (A) =  $-x + 1, -y + 1, -z + 1$  for O(1), O(5), and O(6). (b) The 1D linear chain is formed by the croconate bridge with a μ<sub>1,2,4</sub>-bidentate/monodentate coordination mode. (c) A view of the 2D sheets arranged in an ABAB... packing pattern and extended to infinite 3D cross-like-array network.

**Table 4.** Selected Bond Lengths (Å) and Angles (°) for 3 and 4<sup>a</sup>

3		4	
Cu(1)–N(1)	2.009(3)	Cu(2)–N(1)	2.008(2)
Cu(1)–N(2)	2.004(3)	Cu(2)–N(2)	2.011(2)
Cu(1)–O(3)	2.512(3)	Cu(2)–O(3)	2.491(1)
Ni–O(1)	2.048(2)	Cu(1)–O(1)	1.991(1)
Ni–O(5)	2.199(3)	Cu(1)–O(5)	2.418(1)
Ni–O(6)	2.002(2)	Cu(1)–O(6)	1.955(2)
N(2A)–Cu(1)–N(2)	180	N(2)–Cu(2)–N(2A)	180
N(1)–Cu(2)–N(2)	84.8(2)	N(1)–Cu(2)–N(2)	84.74(9)
N(1A)–Cu(2)–N(2)	95.2(2)	N(1A)–Cu(2)–N(2)	95.26(9)
N(1)–Cu(1)–N(1A)	180	N(1)–Cu(2)–N(1A)	180
O(6A)–Ni(1)–O(6)	180	O(6A)–Cu(1)–O(6)	180
O(6A)–Ni(1)–O(1)	87.9(1)	O(6A)–Cu(1)–O(1)	88.68(6)
O(6)–Ni(1)–O(1)	92.1(1)	O(6)–Cu(1)–O(1)	91.32(6)
O(1)–Ni(1)–O(1A)	180	O(1)–Cu(1)–O(1A)	180
O(6)–Ni(1)–O(5)	87.4(1)	O(6)–Cu(1)–O(5)	87.29(6)
O(6)–Ni(1)–O(5A)	92.6(1)	O(6)–Cu(1)–O(5A)	92.71(6)
O(1)–Cu(1)–O(5)	82.02(9)	O(1)–Cu(1)–O(5)	79.48(5)
O(1)–Cu(1)–O(5A)	97.98(9)	O(1)–Cu(1)–O(5A)	100.52(5)
O(5A)–Ni(1)–O(5)	180	O(5)–Cu(1)–O(5A)	180

<sup>a</sup> Symmetry code: (A) =  $-x + 2, -y, -z + 1$  for N(1) and N(2); (A) =  $-x + 1, -y + 1, -z + 1$  for O(1), O(5), and O(6).

π...π stacking distances.<sup>30,31</sup> The hydrogen bonds resulting from alternate polymeric chains is the second factor for the construction of their 3D packing. The common hydrogen-

**Table 5.** π–π Interactions (Face-to-Face) of Croconate Rings in Compounds 1–6<sup>a</sup>

ring(i) → ring(j)	slip angle <sup>b</sup> (i,j)/°	interplanar (i,j) distance <sup>c</sup> / Å	horizontal shift between the (i,j) ring centroids <sup>d</sup> /Å	distance between the (i,j) ring centroids/Å
1 R(1) → R(1) <sub>i</sub>	23.23	3.369	1.446	3.666
R(1) → R(1) <sub>ii</sub>	21.52	3.404	1.345	3.666
2 R(1) → R(1) <sub>iii</sub>	20.67	3.358	1.267	3.589
R(1) → R(1) <sub>iv</sub>	29.60	3.268	1.856	3.758
3 R(1) → R(1) <sub>v</sub>	21.77	3.388	1.353	3.648
R(1) → R(1) <sub>vi</sub>	23.30	3.350	1.443	3.648
4 R(1) → R(1) <sub>v</sub>	21.69	3.346	1.331	3.601
R(1) → R(1) <sub>vi</sub>	20.01	3.384	1.232	3.601
5 R(1) → R(1) <sub>vii</sub>	20.14	3.388	1.242	3.608
R(1) → R(1) <sub>viii</sub>	30.18	3.293	1.915	3.809
6 R(1) → R(1) <sub>viii</sub>	21.35	3.868	1.512	4.153
R(1) → R(1) <sub>viii</sub>	37.12	3.365	2.547	4.220

<sup>a</sup> Symmetry code: (i) =  $x, -y + 1/2, z + 1/2$ ; (ii) =  $x, -y + 1/2, z - 1/2$ ; (iii) =  $-x + 1, -y, -z + 1$ ; (iv) =  $-x, -y, -z + 1$ ; (v) =  $x, -y + 1/2, z + 1/2$ ; (vi) =  $x, -y + 1/2, z - 1/2$ ; (vii) =  $-x, -y + 2, -z + 1$ ; (viii) =  $-x + 1, -y + 2, -z + 1$ . R(i)/R(j) denotes the centroids of ith/jth of croconate/croconate; R(1) = C(1)–C(2)–C(3)–C(4)–C(5). <sup>b</sup> Slip angle: the angle formed between the ring-centroid vector (CC) and the ring normal to one of the croconate planes. <sup>c</sup> Interplanar distance: the perpendicular distance between two parallel croconate rings. <sup>d</sup> Horizontal shift between the ring centroids: a shift from the face-to-face alignment.

bonding distances and angles existing in 1, 2, and 3 & 4, are in STable 1, 2, and 3, Supporting Information, respectively. It is important to note that the N–H...O and O–H...O hydrogen bonding interactions are formed through the uncoordinated oxygen atoms (O(2), O(3), and O(5) in 1, O(4) and O(5) in 2 & 5, O(2) and O(4) in 3 & 4) of croconate ligands interacting with the ethylenediamine (en) and coordinated water ligands, respectively. The N...O and O...O distances are in the range of 3.031–3.293 and 2.674–2.728 Å, respectively. These hydrogen-bonding interactions facilitate the formation of 2D sheet (Figures 1c, 2c, and 3c) in an ABAB... packing pattern and are then extended to an infinite 3D cross-like-array network. Their overall 3D architectures are further reinforced by N–H...O and O–H...O hydrogen bonding among the solvated, coordinated water molecules, and en ligands. The shortest interchain M...Cu and M...M (or Cu...Cu) separations are 6.795 and 7.010 Å for 1, 5.631 and 7.159 for 2, 5.623 and 7.074 for 3, 5.692 and 7.010 for 4, and 5.609 and 7.219 Å, for 5, respectively.

[Cu(C<sub>5</sub>O<sub>5</sub>)(en)(H<sub>2</sub>O)]<sub>2</sub> (6). Figure 4 shows the ORTEP view of the centrosymmetric neutral dimer [Cu(C<sub>5</sub>O<sub>5</sub>)(en)(H<sub>2</sub>O)]<sub>2</sub>, together with the atom labeling scheme. Selected bond lengths and angles around the copper atom are given in Table 6. It is made of two croconate ligands acting as a unprecedented μ<sub>1,1,2</sub>-coordination mode (Scheme 1d) to bridge two copper atoms with a separation distance of 3.57 Å. Each copper atom is involved in a tetragonally elongated distorted octahedral CuN<sub>2</sub>O<sub>4</sub> environment bonded to two en N atoms with Cu–N bond distances of 1.993(2) and 1.988(2) Å and two oxygen atoms (bridging O(1) and O(5)) of one chelated croconate with Cu–O bond distances of 2.020(1) and 2.363(2) Å, one bridging oxygen (O(1))\* indicates a symmetry operation of  $1 - x, 3 - y, 2 - z$  of a second croconate with a longer Cu–O bond distance of 2.553(2) Å and one water molecule (O(6)) with a Cu–O bond distance of 2.015(2) Å. It is also interesting to note that the crystal packing shows layers of dimeric complexes, which are held together by means of an extended network of the combination of π...π stacking and hydrogen-bonding interactions, parallel to the yz plane (Figure 4b). The croconate ligands of adjacent dimers are superimposed (Figure 4b) such that the croconates stack on each other with distances of 4.153 and 4.220 Å between the ring centroids (Table 5). The hydrogen bond is



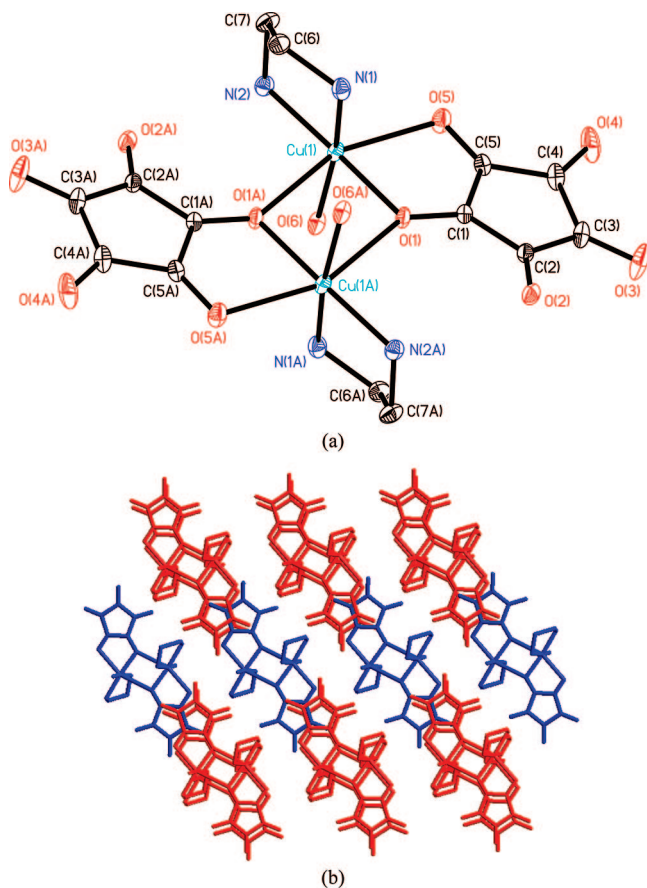


**Figure 4.** (a) ORTEP drawing for the asymmetric unit of  $[\text{Cu}(\text{C}_5\text{O}_5)(\text{en})(\text{H}_2\text{O})]_2$  dimer, showing 30% probability ellipsoids. Symmetry code: (A) =  $1 - x, 3 - y, 2 - z$ . (b) A view of the layered structure of **6** through  $\pi$ - $\pi$  and hydrogen bonding interaction.

**Table 6.** Selected Bond Lengths (Å) and Angles (°) for **6<sup>a</sup>**

Cu–N(1)	1.993(2)	Cu–N(2)	1.988(2)
Cu(1)–O(1)	2.020(1)	Cu(1)–O(6)	2.015(2)
Cu(1)–O(5)	2.363(2)	Cu(1)–O(1A)	2.553(2)
N(2)–Cu(1)–N(1)	85.61(8)	O(6)–Cu(1)–O(1)	90.09(7)
N(2)–Cu(1)–O(6)	93.89(8)	N(2)–Cu(1)–O(5)	105.82(7)
N(1)–Cu(1)–O(6)	170.18(9)	N(1)–Cu(1)–O(5)	99.08(8)
N(2)–Cu(1)–O(1)	173.68(7)	O(6)–Cu(1)–O(5)	90.50(7)
N(1)–Cu(1)–O(1)	89.63(7)	O(1)–Cu(1)–O(5)	79.03(5)

<sup>a</sup> Symmetry code: (A) =  $1 - x, 3 - y, 2 - z$ .

the other important factor for the construction of its 3D packing. The common hydrogen-bonding distances and angles existing in **6** are summarized in Table 10S, Supporting Information. The N–H $\cdots$ O and O–H $\cdots$ O hydrogen bonding interactions are formed through the uncoordinated oxygen atoms (O(2), O(3) and O(4)) of croconate ligands interacting with the ethylenediamine (en) and coordinated water ligands, respectively. The N $\cdots$ O and O $\cdots$ O distances are in the range of 2.984–3.335 and 2.721–2.853 Å, respectively.

**Thermogravimetric Analysis and in Situ Powder X-ray Diffraction Measurement.** To assess the thermal stability of compounds **1–6** and their structural variation as a function of the temperature, thermogravimetric analyses (TGA) were performed on single-phase polycrystalline samples of each compound. During the heating process, TGA (shown in SFigure 1a, Supporting Information) shows that the two-step weight loss of 11.10% and 3.74% for **1**, corresponding to the lost of crystallized water (calc 11.95%) and coordinated water (calc

2.99%), respectively, occurred in the range of approximate 50–73 °C and 103–117 °C. On further heating, the samples decomposed at approximately 140–300 °C with a weight loss of 58.13%. For compounds **2–6**, all underwent a continuous multi-step weight loss process (shown in SFigure 2a to SFigure 6a, Supporting Information) and were thermally stable up to 140, 90, 80, 120, and 120 °C for **2**, **3**, **4**, **5**, and **6**, respectively. In situ powder X-ray diffraction was carried out for compounds **1–6** by synchrotron X-rays (shown in SFigure 1b to SFigure 6b, Supporting Information). The crystal structures of compounds **1–6** are thermally stable at a temperature below 150 °C. No phase transition was found for compounds **2–6** during the water adsorption process, except for compound **1**. On further heating, the samples decomposed at about 300–400 °C for all compounds **1–6**. Above 400 °C, compounds **1–6** all decomposed completely, and the final products of the pyrolysis were either pure metals or metal oxides according to JCPDS files, and no alloy or bimetallic compound was found.

## Conclusions

Five supramolecular coordination polymers containing  $[\text{M}(\text{C}_5\text{O}_5)_2(\text{H}_2\text{O})_n]^{2-}$  have been prepared, indicating that  $[\text{M}(\text{C}_5\text{O}_5)_2(\text{H}_2\text{O})_n]^{2-}$  may serve as a useful building unit in the preparation of coordination polymers. The polyfunctional croconate ligand plays an important role not only in the construction of 1D linear or zigzag chain-like coordination polymers with three types of bridging modes,  $\mu_{1,3}$ -bis-monodentate,  $\mu_{1,2,3}$ -, and  $\mu_{1,2,4}$ -bidentate/monodentate coordination modes, but also on the structural extension to the 3D supramolecular array by the combination of  $\pi\cdots\pi$  stacking between croconate and hydrogen-bonding interactions among the croconate, en, and  $\text{H}_2\text{O}$ .

**Acknowledgment.** The authors acknowledge the National Science Council (NSC), Taiwan ROC, for financial support.

**Supporting Information Available:** Hydrogen-bond distances (Å) and angles (deg) in **1–6** (Tables S1–S4), thermogravimetric analyses and in-situ synchrotron powder X-ray diffraction patterns (SFigure 1 to SFigure 6) for **1–6** and CIF files of the six structures of **1–6**. This material is available free of charge via the Internet at <http://pubs.acs.org>.

## References

- (1) (a) Janiak, C. *Dalton Trans.* **2003**, 2781–2804. (b) James, S. L. *Chem. Soc. Rev.* **2003**, 32, 276. (c) Mueller, U.; Schubert, M.; Teich, F.; Puetter, H.; Schierle-Arndt, K.; Pastré, J. J. *Mater. Chem.* **2006**, 16, 626. (d) Champness, N. R. *Dalton Trans.* **2006**, 877. (e) Lin, X.; Jia, J.; Hubbert, P.; Schröder, M.; Champness, N. R. *CrystEngComm* **2007**, 9, 438. (f) Janiak, C. *Angew. Chem., Int. Ed.* **1997**, 36, 1431.
- (2) (a) Kesanli, B.; Lin, W. *Coord. Chem. Rev.* **2003**, 246, 305. (b) Cahill, C. L.; de Lill, D. T.; Frisch, M. *CrystEngComm* **2007**, 9, 15. (c) Zhou, Y.; Hong, M.; Wu, X. *Chem. Commun.* **2006**, 135. (d) Zheng, S.-L.; Chen, X.-M. *Aust. J. Chem.* **2004**, 57, 703. (e) Maspoch, D.; Ruiz-Molina, D.; Veciana, J. *Chem. Soc. Rev.* **2007**, 36, 770. (f) Maspoch, D.; Ruiz-Molina, D.; Veciana, J. *J. Mater. Chem.* **2004**, 14, 2713. (g) Batten, S. R.; Murray, K. S. *Coord. Chem. Rev.* **2003**, 246, 103. (h) Férey, G. *Chem. Soc. Rev.* **2008**, 37, 191. (i) Kitagawa, S.; Noro, S.-I.; Nakamura, T. *Chem. Commun.* **2006**, 701. (j) Kepert, C. J. *Chem. Commun.* **2006**, 695. (k) Kitagawa, S.; Uemura, K. *Chem. Soc. Rev.* **2005**, 34, 109.
- (3) (a) Ohba, M.; Okawa, H. *Coord. Chem. Rev.* **2000**, 198, 313. (b) Ohba, M.; Usuki, N.; Fukita, N.; Okawa, H. *Angew. Chem., Int. Ed.* **1999**, 38, 1795. (c) Ohba, M.; Usuki, N.; Fukita, N.; Okawa, H. *Inorg. Chem.* **1998**, 37, 3349. (d) Ohba, M.; Okawa, H.; Fukita, N.; Hashimoto, Y. *J. Am. Chem. Soc.* **1997**, 119, 1011.
- (4) (a) Dunbar, K. R.; Heintz, R. A. *Prog. Inorg. Chem.* **1997**, 45, 2283, and references therein. (b) Yuan, A.; Zou, J.; Li, B.; Zha, Z.; Duan, C.; Liu, Y.; Xu, Z.; Keizer, S. *Chem. Commun.* **2000**, 1297. (c)



- Shorrock, C. J.; Jong, H.; Batchelor, R. J.; Leznoff, D. B. *Inorg. Chem.* **2003**, 423917.
- (5) (a) Castro, I.; Sletten, J.; Faus, J.; Julve, M. *J. Chem. Soc., Dalton Trans.* **1992**, 2271. (b) Carranza, J.; Brennan, C.; Sletten, J.; Vangdal, B.; Rillema, P.; Lloret, F.; Julve, M. *New J. Chem.* **2003**, 27, 1775. (c) Carranza, J.; Sletten, J.; Brennan, C.; Lloret, F.; Cano, J.; Julve, M. *Dalton Trans.* **2004**, 3997. (d) Calatayud, M. L.; Sletten, J.; Julve, M.; Castro, I. *J. Mol. Struct.* **2005**, 741, 121.
- (6) Glick, M. D.; Downs, G. L.; Dahl, L. F. *Inorg. Chem.* **1964**, 3, 1712.
- (7) Castan, P.; Deguenon, D.; Dahan, F. *Acta Crystallogr., Sect. C* **1991**, 47, 2656.
- (8) Castro, I.; Sletten, J.; Glærum, L. K.; Lloret, F.; Faus, J.; Julve, M. *J. Chem. Soc., Dalton Trans.* **1994**, 2777.
- (9) Sletten, J.; Bjørsvik, O. *Acta Chem. Scand.* **1998**, 32, 770.
- (10) Deguenon, D.; Castan, P.; Dahan, F. *Acta Crystallogr., Sect. C* **1991**, 47, 433.
- (11) Deguenon, D.; Bernardelli, G.; Tuchagues, J. P.; Castan, P. *Inorg. Chem.* **1990**, 29, 3031.
- (12) Chen, Q.; Liu, S.; Zubietta, J. *Inorg. Chim. Acta* **1990**, 175, 241.
- (13) Wang, C. C.; Yang, C. H.; Lee, G. H. *Inorg. Chem.* **2002**, 41, 1015.
- (14) Glick, M. D.; Dahl, L. F. *Inorg. Chem.* **1966**, 5, 289.
- (15) Cornia, A.; Fabretti, A. C.; Giusti, A.; Ferraro, F.; Gatteschi, D. *Inorg. Chim. Acta* **1993**, 212, 87.
- (16) Castro, I.; Sletten, J.; Faus, J.; Julve, M.; Journaux, Y.; Lloret, F.; Alvarez, S. *Inorg. Chem.* **1992**, 31, 1889.
- (17) Castro, I.; Calatayud, M. L.; Lloret, F.; Sletten, J.; Julve, M. *J. Chem. Soc., Dalton Trans.* **2002**, 2397.
- (18) (a) Wang, C. C.; Yang, C. H.; Tseng, S. M.; Lee, G.-H.; Chiang, Y.-P.; Sheu, H. S. *Inorg. Chem.* **2003**, 42, 8294. (b) Wang, C. C.; Lin, H.-W.; Yang, C. H.; Liao, C. H.; Lan, I. T.; Lee, G. H. *New J. Chem.* **2004**, 28, 180. (c) Wang, C. C.; Tseng, S. M.; Lin, S. Y.; Liu, F. C.; Dai, S. C.; Lee, G. H.; Shih, W. J.; Sheu, H. S. *Cryst. Growth Des.* **2007**, 7, 1783. (d) Wang, C. C.; Dai, S. C.; Lin, H. W.; Lee, G. H.; Sheu, H. S.; Lin, Y. H.; Tsai, H. L. *Inorg. Chim. Acta* **2007**, 360, 4058.
- (19) Castro, I.; Calatayud, M. L.; Sletten, J.; Julve, M.; Lloret, F. C. R. *Acad. Sci. Paris, Chim.* **2001**, 4, 235.
- (20) Maji, T. K.; Konar, S.; Mostafa, G.; Zangrando, E.; Lu, T. H.; Chaudhuri, N. R. *J. Chem. Soc., Dalton Trans.* **2003**, 171.
- (21) Ghoshal, D.; Ghosh, A. K.; Ribas, J.; Mostafa, G.; Chaudhuri, N. R. *CrystEngComm* **2005**, 7, 616.
- (22) Das, N.; Ghosh, A.; Arif, A. M.; Stang, P. J. *Inorg. Chem.* **2005**, 44, 7130.
- (23) Maji, T. K.; Ghoshal, D.; Zangrando, E.; Ribas, J.; Chaudhuri, N. R. *CrystEngComm* **2004**, 6, 623.
- (24) Wang, C. C.; Kuo, C. T.; Yang, J. C.; Lee, G. H.; Shih, W. J.; Sheu, H. S. *Cryst. Growth Des.* **2007**, 7, 1476.
- (25) Habib, H. A.; Sanchiz, J.; Janiak, C. *Dalton Trans.* **2008**, 1734, and references therein.
- (26) (a) SMART V 4.043 Software for the CCD Detector System; Siemens Analytical Instruments Division: Madison, WI, 1995. (b) SAINT V 4.035 Software for the CCD Detector System; Siemens Analytical Instruments Division: Madison, WI, 1995.
- (27) Sheldrick, G. M. *SHELXL-93, Program for the Refinement of Crystal Structures*; University of Göttingen: Göttingen, Germany, 1993.
- (28) *SHELXTL 5.03 (PC-Version), Program Library for Structure Solution and Molecular Graphics*; Siemens Analytical Instruments Division: Madison, WI, 1995.
- (29) Ito, M.; Weiss, R. *J. Am. Chem. Soc.* **1963**, 85, 2580.
- (30) (a) Janiak, C. *J. Chem. Soc., Dalton Trans.* **2000**, 3885. (b) Ghoshal, D.; Maji, T. K.; Mostafa, G.; Lu, T.; Chaudhuri, N. R. *Cryst. Growth Des.* **2003**, 3, 9. (c) Lehn, J.-M. *Supramolecular Chemistry*; VCH: Weinheim, 1995. (d) Lehn, J.-M. *Angew. Chem., Int. Ed. Engl.* **1990**, 29, 1304. (e) Hargman, P. J.; Hargman, D.; Zubietta, J. *Angew. Chem., Int. Ed.* **1999**, 38, 2638. (f) Brunsveld, L.; Meijer, E. W.; Prince, R. B.; Moore, J. S. *J. Am. Chem. Soc.* **2001**, 123, 7978. (g) Ko, J. W.; Min, K. S.; Suh, M. P. *Inorg. Chem.* **2002**, 41, 2151.
- (31) Braga, D.; Maini, L.; Grepioni, F. *Chem. Eur. J.* **2002**, 8, 1804.

CG800827A